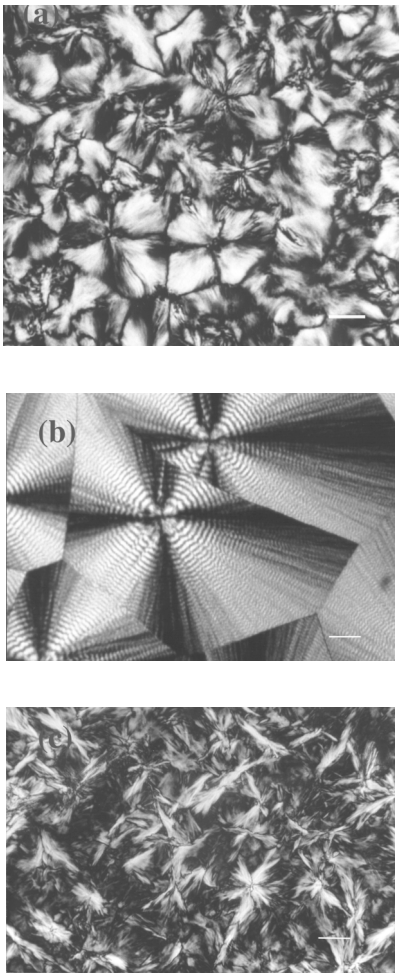

Fig. 6.16. Polarized photomicrographs of different linear polyethylenes showing (a) non-banded spherulites; (b) banded spherulites (from ref. 114 with permission from Elsevier, UK); (c) axialites. Scale bars represent 20 µm.

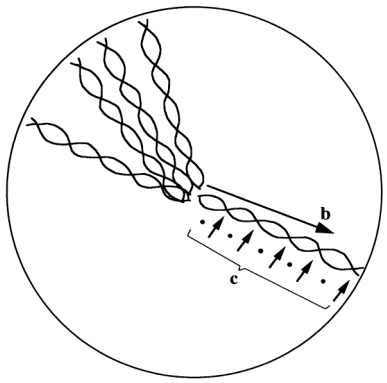

Fig. 6.17. Schematic (simplified) representation of twisting lamella radiating out from the centre of a banded spherulite.

It is important to point out that several different superstructures are formed in polyethylene depending on the molar mass of the polymer and the crystallization temperature (Fig. 6.16). Linear polyethylenes (narrow molar mass distribution; $\overline{M}_w/\overline{M}_n \approx 1.1$) of molar mass between 18 000 and 115 000 g mol^{-1} form negative spherulites on crystallization at 17.5°C or greater degrees of supercooling (45). Keller (108) and Point (109) showed independently that the crystallographic **b** axis was mainly along the spherulite radius, whereas the chain axis is preferentially oriented in the tangential plane of the spherulites. Banded spherulites – the optical texture is concentric rings overlapping the Maltese cross – are formed on crystallization at low temperatures, typically at 20-25°C or higher degree of supercooling. Banded polyethylene spherulites were first reported by Keller (110). Keith and Padden (111,112) related this periodic structure to the periodic twisting of the crystal lamellae earlier observed by Fischer (28). Hence, while the **b** axis is along the radius, the **c** axis shows a periodic twisting in the transverse plane along the spherulite radius (Fig. 6.17). Keller (113) showed that the band period decreases with decreasing crystallization temperature. More recently Rego Lopez and Gedde (114) reported for a narrow fraction of linear polyethylene ($\overline{M}_w$= 66 000 g mol^{-1}; $\overline{M}_w/\overline{M}_n$ =1.2) the following formation temperatures for the different spherulitic structures: non-banded spherulites: 121.5-127.5°C; banded (5-10 μm band period) spherulites: 118-121.5°C; banded (2-5 μm band period) spherulites: 114-118°C; banded (1-2 μm band period) spherulites: 110.5-114°C; banded (< 1 μm band period) spherulites: < 110.5°C.

Crystallization at higher temperatures (degree of supercooling ≤ 17.5°C) of linear polyethylene fractions of molar masses between 18 000 and 115 000 g mol^{-1} yields axialites (45). Low molar mass linear polyethylenes (M< 17 000 g mol^{-1}) form axialites at all crystallization temperatures (45). It seems thus the mechanism(s) leading to the multiplication and splaying of the growing crystal lamellae occurs less frequently at higher crystallization temperatures.

Linear polyethylene fractions ($\overline{M}_w/\overline{M}_n$ =1.26-1.81) in the molar mass range 119 000 to 800 000 g mol^{-1} crystallize also at high temperatures in spherulites; Hoffman et al. (45) refer to these as 'irregular' spherulites.

Very high molar mass polyethylene (M≥ 2 000 000 g mol^{-1}) crystallizes without the formation of a clear superstructure, sometimes referred to as the random lamellar structure (115). The great many chain entanglements present in high molar mass polymers obstruct crystallization and the crystals become small and their orientation less correlated with surrounding crystal lamellae.

Our understanding of the lamellar structure underlying the different superstructures is based on studies by transmission electron microscopy of replicates or stained thin sections. The early studies of Anderson (116) and Mandelkern et al. (117) on

replicates of fracture surfaces provided the view along the **a** axis with the **b** axis (i.e. the spherulite radius) in the fracture surface plane (118). Complementary information was obtained from studies of sections stained with chlorosulphonic acid according to the method developed by Kanig (119). This technique permits a clear view only of crystal lamellae with their lamella normal perpendicular to the electron beam (i.e. 'edge on'), see Fig. 6.18. Tilted lamellae appear less sharp and areas without lamellar contrast are found over large areas in the electron micrographs (120). The location of the sections should be at random with respect to the centres of the spherulites. From simple geometrical considerations, it can be shown that the average distance between the section and the spherulite centre should be $R/\sqrt{3}$ where R is the radius of the spherulite. It is well established that the **b** axis is parallel to the radius of a mature spherulite. Hence, sharply appearing crystal lamellae are dominantly viewed along **b** which must be only a limited area of the section: 40% of the surface is within a 20° angle from the spherulite radius and 60% within a 30° angle from the spherulite radius.

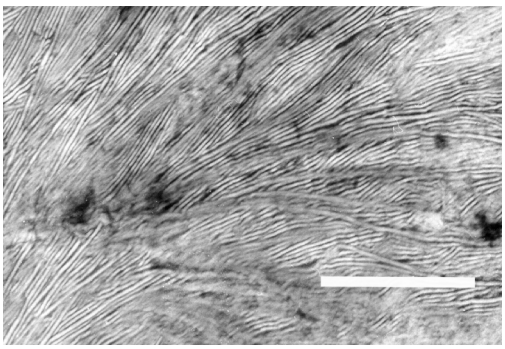

Fig. 6.18. Transmission electron micrograph of a chlorosulphonated section of polyethylene. Scale bar represents 0.5 µm. Courtesy of M. T. Conde Braña.

The permanganic etching technique using solutions prepared from H_2SO_4 and $KMnO_4$ was introduced by Olley et al. (121). This paper was submitted already in 1977 but the paper by Bassett and Hodge (118) showing electron micrographs of replicates of samples treated with the permanganic etching technique was published first. The permanganic etching technique has been developed further by reducing the concentration of $KMnO_4$ from 7% to between 0.7 and 2% and by introducing orthophosphoric acid in order to avoid the formation of artificial structures observed primarily at low magnification. The acid etches to a depth of 1-2 μm and the crystal lamellae can be observed at all the angles with respect to their crystallographic axes (118). Hence, the method provides edge-on-views of the crystals along the **b** axis and views along **c** revealing the lateral habit (Fig. 6.19). The morphology of individual

crystal lamellae, mainly views along the lamellar normal, were obtained by depositing dilute solutions of polyethylene on freshly cleaved mica, evaporating the solvent, crystallizing the melt and shadowing (105). It should be noted that the crystals revealed in this case are not from a true three-dimensional spherulite.

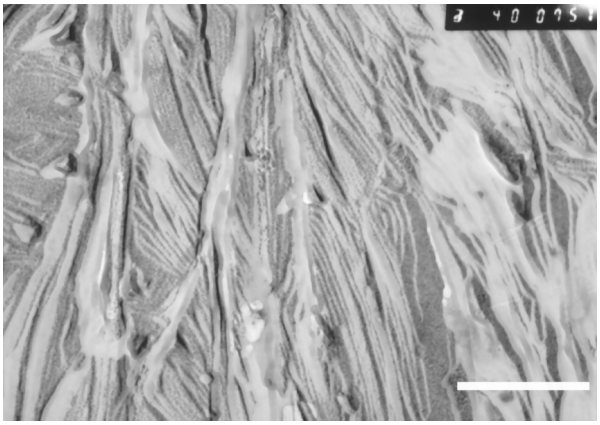

Fig. 6.19. Transmission electron micrograph of a replicate of permanganic-etched polyethylene. Scale bar represents 0.5 µm. Courtesy of M. T. Conde Braña.

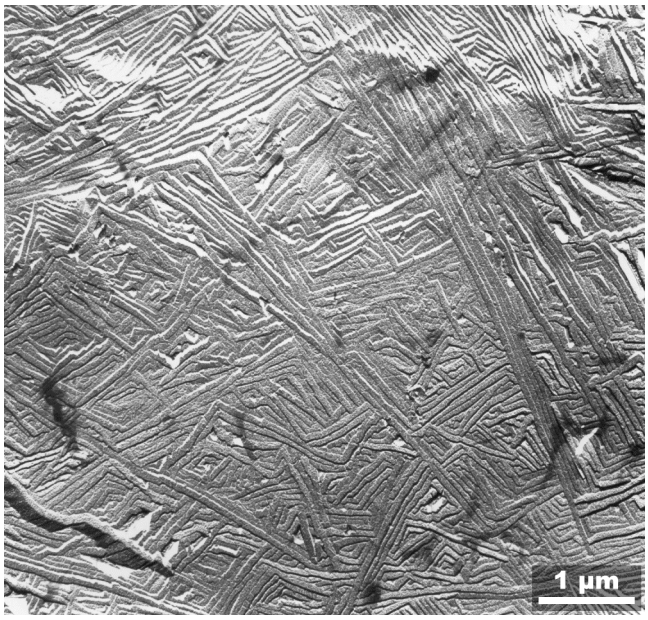

Fig. 6.20. Transmission electron micrograph of permanganic-etched linear polyethylene fraction crystallized at 130.4°C for 27 days. Courtesy of D. C. Bassett. From ref. (46) with permission from the Royal Society of London, UK.

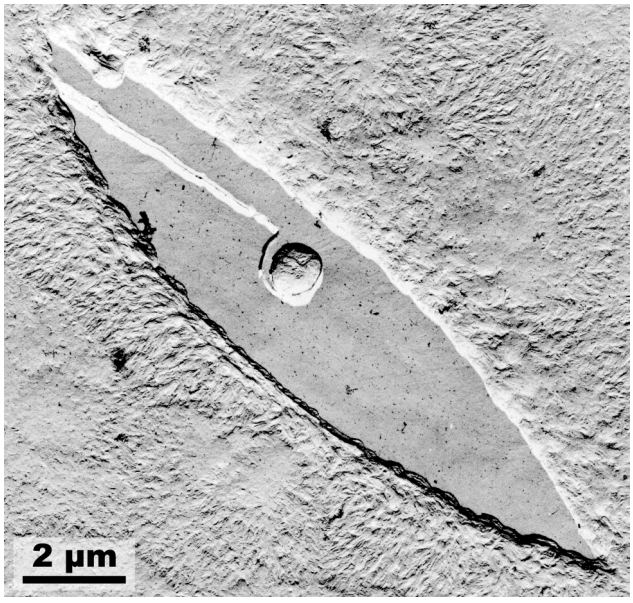

Fig. 6.21. Transmission electron micrograph of permanganic-etched linear polyethylene ($\overline{M}_n$ = 17 000 g mol^{-1}; $\overline{M}_w$ = 54 000 g mol^{-1}) crystallized at 130°C for 13 h showing a lenticular crystal lamella. Courtesy of D. C. Bassett. From ref. (54) with permission from Elsevier, UK.

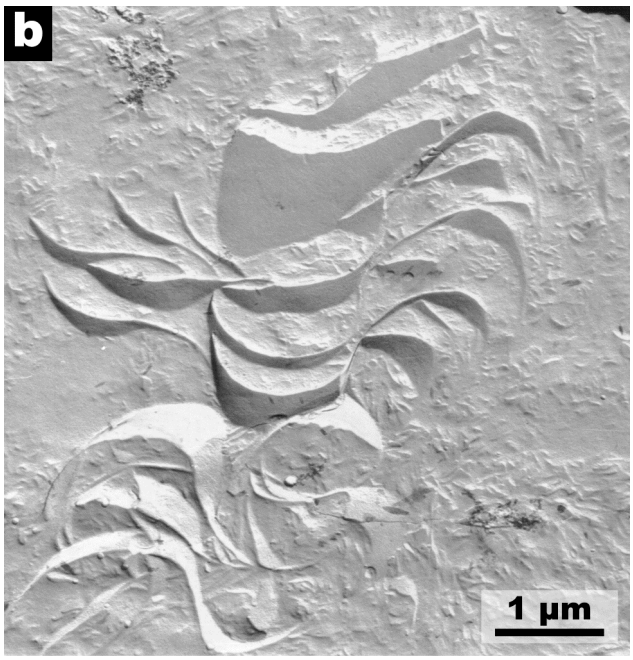

Fig. 6.22. Transmission electron micrograph of permanganic-etched branched polyethylene crystallized at 120°C for 1 min showing dominant S-shaped lamellae. From Patel and Bassett (54) with permission from Elsevier, UK.

Let us start by looking at the lamellar morphology viewed along the radius of the spherulite (axialite). The general picture of the dominant crystal lamellae morphology was provided already in 1981 by Bassett et al. (107) who studied a wide range of linear polyethylenes including fractions after crystallization at 120 to 131°C. Crystallization at 130°C of the low molar mass samples (20 000-50 000 g mol^{-1}) yielded both planar sheets and ridged sheets, both 4 μm wide as viewed along the **b** axis (Fig. 6.20). Later studies by Keith et al. (105), Toda (106) and Toda and Keller (37) of melt-grown single-crystal linear polyethylenes in this molar range were in principle in accordance with the findings of Bassett et al. (46). The lenticular single crystals shown in Fig. 6.21 were reported to be flat, with a 35° chain tilt angle corresponding to a fold surface close to {201}, and one of the studies (105) reported an asymmetric lateral habit that was suggested to be related to the fact that the chains were inclined so that the growth rate was slower on the side with overhanging folds and cilia. The fraction of planar sheets increased with increasing molar mass in this molar mass range. Higher molar mass polyethylenes (>100 000 g mol^{-1}) crystallizing at 130°C showed curved lamellae and occasional ridged and planar lamellae viewed along **b**. The maximum width of these structures from the **b** view was 4 μm. Bassett et al. (46) reported further that the structures at 128°C were similar to those found at 130°C except that the ridged sheets were not found in the low molar mass samples. Crystallization at 125°C resulted in dominantly curved and S-shaped lamellae except for the sample with the lowest molar mass ($M\approx$ 20 000 g mol^{-1}), which still showed planar lamellae. The latter sample after crystallization at 120°C showed mostly S-shaped dominant lamellae but still with a few planar sheets (46). The main conclusion drawn by Bassett et al. (46) was that the lamellar profile viewed along **b** is planar or ridged for axialites and curved (C- or S-shaped) for spherulites (Fig. 6.22). The angle between the lamellar normal and **c** of the S-shaped crystals changed continuously along the crystal with a maximum of 35°. Toda (106) revealed the lateral habit for melt-grown crystals of a linear polyethylene fraction ($\overline{M}_w$= 32 000 g mol^{-1}) formed at temperatures between 125 and 130°C. The crystals grown within the Regime II temperature region (<128°C) were basically truncated lozenges with rounded {100} and {110} faces. These crystals were also less extended along **b**. In a subsequent study, Toda and Keller (37) reported that these crystals were chair-like. In a view along **b** these crystals appear curved. It is pointed out by the authors that the chair-like crystals are curved in the opposite way to Bassett's S-shaped lamellae, i.e. they constitute a new class of curved lamellae. It is suggested that the restructuring of the fold surface is the fundamental reason for the different observed shapes of the crystal lamellae as viewed along **b**. The idea of an initial irregular and short-lived fold surface is relatively old (122,123), but direct evidence came by the paper of Ungar

and Keller (53). Abo el Maaty and Bassett (124) found by electron microscopy that the initial (disordered) structure was non-inclined, i.e. the crystal stems were parallel to the lamellar normal. This structure is only temporary and it rearranges into a more ordered and inclined (tilt angle ~35°) fold structure. Abo el Maaty and Bassett (124) proposed that the different crystal shapes as viewed along **b** are a consequence of the relative rates of fold surface ordering and the advance of crystal front. The rate of advance of the crystal front should be proportional to exp $[-K_g/(T_c\Delta T)]$, i.e. it decreases strongly with increasing temperature (45), whereas the rate of fold surface ordering may even be faster at higher temperatures. The most 'efficient' mechanism for a longitudinal shift of stems – a process that must be important for the fold surface ordering – is by the α process, which shows an Arrhenius temperature dependence, i.e. the rate is proportional to exp $[-\Delta E/(RT_c)]$ (21). The discovery by Abo el Maaty and Bassett (124) that high temperature crystallization (>127°C) led to immediate fold surface ordering and the formation of planar sheets with an inclined (35° tilt angle) fold surface is thus logical. Crystallization at lower temperatures led according to electron microscopy findings to the formation to a more long-lived planar lamellar structure with non-inclined fold surfaces. The transformation to the more energetically favourable inclined {201} fold surface occurred at a later stage behind the crystal front (124). This means that the fold surface ordering (chain tilting) occurs within a lamella with a non-inclined 'outer' part which provides some constraint on the process. The stresses built up in such lamella trigger the deformation of the initially plane sheets to the S-shape. Abo el Maaty and Bassett (124) suggested that the S-shape is more easily adapted in more open textures with a low degree of crystallinity.

The length of the crystals along the spherulite (axialite) radius is not easily determined from electron micrographs because of lamellar branching and because the view is seldom perpendicular to the spherulite radius. Bassett and Hodge (118) reported, however, that they traced individual crystals over 20 μm, which was a very significant part of the spherulite radius in the particular case. There seems to be a consensus that the crystals are continuous from the centre to the periphery of the spherulites. The implication of the lamellar branching, as will be discussed in the next paragraph, is that the individual crystal lamella is a highly branched structure. It starts as a single sheet but it soon branches into many growth faces which are continuous at the periphery of the spherulite.

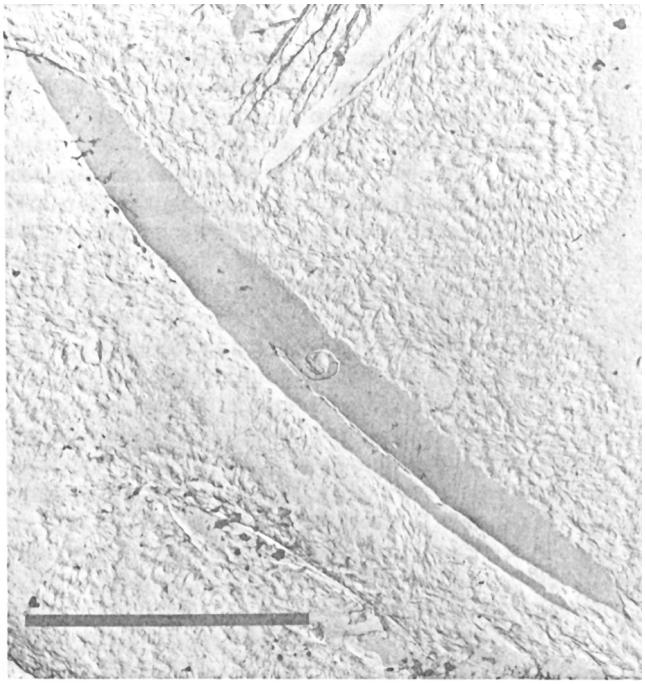

(b)

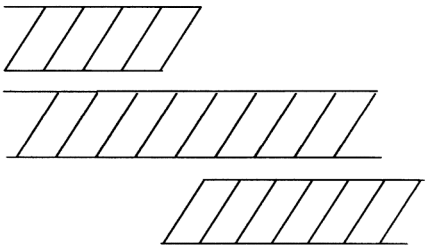

Fig. 6.23. (a) Transmission electron micrograph of permanganic-etched linear polyethylene. The micrograph shows the spiral development around a screw dislocation in a sample crystallised at 130°C. Scale bar represents 10 µm. Courtesy of D. C. Bassett. From ref. (104) with permission from Elsevier, UK. (b) Sketch showing ***c*** *with respect to the fold surface of the crystal layers around the screw dislocation.*

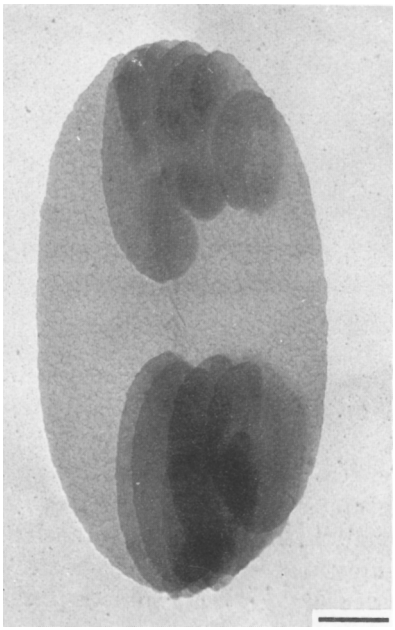

Fig. 6.24. Transmission electron micrograph of linear polyethylene crystallized at 127°C for 2.5 min showing spiral terraces in the {110} sectors. Scale bar represents 1 µm. From Toda and Keller (37) with permission from Springer Verlag, Germany.

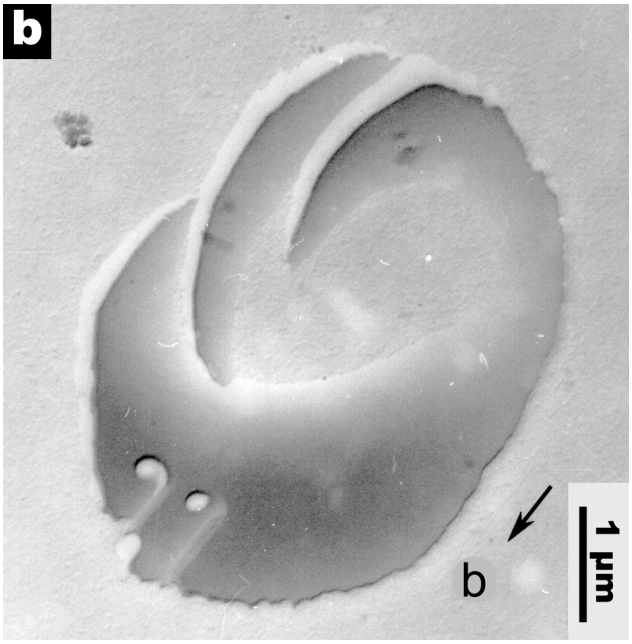

Fig. 6.25. Transmission electron micrograph of permanganic-etched branched polyethylene crystallized at 123°C for 35 min. From Patel and Bassett (54) with permission from Elsevier, UK.

Let us now consider about how more crystals are created during the course of crystallization from the centre towards the periphery of the spherulite. Historically,

non-crystallographic branching and self-epitaxy must be mentioned. The first mechanism means that the crystallographic regularity is broken between the mother and daughter crystals and that the latter can grow at any angle with respect to the mother crystal. Self-epitaxy, most prominent in the crosshatched morphology of isotactic polypropylene with the α-crystal phase, means that the chains are nucleating in a particular, well-defined manner on the surface of the mother crystal. Self-epitaxy occurs at a specific angle with respect to the mother crystal. A third possibility, a crystallographic branching that not only provides the required multiplication effect but also causes splaying of mother and daughter crystals, has been demonstrated by Bassett (125), Bassett and Olley (126) and Bassett and Vaughan (127), who observed splaying dominant lamellae with a certain angle of divergence, ~20°. Bassett (125) argued on the basis of these results from studies of strictly monodisperse n-alkanes that the reason for the splaying of the crystals is 'ciliation'. During the process of attachment of stems to the growth surface of a growing crystal, the remaining uncrystallized part of a single chain is in the form of a cilium. This phenomenon is referred to as transient ciliation. The ensemble of cilia in the vicinity of the contact point should generate a positive internal pressure that makes the crystal arms to diverge by an angle of approximately 20°. Direct evidence of lamellar branching was reported for linear polyethylene by Bassett et al. (104). They observed spiral terraces around screw dislocations providing in each branch two growing crystal 'arms' with splaying of these two successive layers (Fig. 6.23). An important discovery reported by these authors was that the upper and lower layers of a three-layer terrace have stopped their growth at the side where their lateral surfaces make an accute angle (angle<90°) to the fold surface of the adjacent layer (Fig. 6.23). This gives the spiral a certain chirality. Further confirmation was delivered by Bassett et al. (128,129) who showed that the crystallization of strictly monochromatic n-alkanes in extended-chain crystals (thus without ciliation) leads to the formation of axialites, which confirms the important role of ciliation in branching/splaying and spherulite formation. The importance of a permanent cilium, i.e. a portion of the polymer chain that preserves its amorphous character even after a long time, on lamellar splaying was recognized by Techoe and Bassett (130) and Hosier and Bassett (131,132). Toda and Keller (37) found that the spiral terraces were mainly in the {110} sectors of the truncated lozenges in the Regime II, i.e. at crystallization temperatures below 127°C (Fig. 6.24). They also noted that the spiral terraces were much less frequent in the lenticular crystals formed in Regime I, i.e. at crystallization temperatures above 127°C. The relatively few lamellar branches created during regime I growth are thus sufficient to achieve spherical symmetry, and hence axialites are formed.

The twisting lamellar structure of banded spherulites has been debated for decades without any satisfactory answer having been obtained until recently. The nature of the isochiral (certain uniform handedness) lamellar twisting and the synchronic character of the twisting of a group of adjacent dominant lamellae both require an explanation. The permanganic etching technique provided the three-dimensional perspective of the structure that was needed to reveal the morphological facts necessary to understand the lamellar structure of banded spherulites. Let us first repeat that the dominant lamellae in banded spherulites are S- or C-shaped as viewed along **b** and that they twist along **b** in a regular (on average) and coordinated fashion. Electron microscopy has identified two different lamellar regions where the twist occurs (107): (1) The spiral terraces generated by screw dislocations are responsible for almost the entire twist. Fig. 6.25 shows a crystal lamella with screw dislocations. Important features are the splaying and the twisting of the branching crystals and the redirection of **b** of the branching crystals with respect to that of the mother crystal. The branching crystals thus form diagonal links in the structure, a feature already found by Bassett and Hodge (107). (2) A much smaller contribution to the twist is that associated with the isochiral twist of the lamellae between the lamellar branches. In fact, the original view of Bassett and Hodge (107) was that these parts of the lamellae were untwisted. However, a more recent paper by Patel and Bassett (54) identifies a small twisting of the lamellae about **b**; 5° over the band period of 1 μm, which means that the angle of 175° originates from the regions near the lamellar branch regions. The circumferential coordination of the lamellar twisting is very obvious from many electron micrographs presented in the literature. What is the fundamental reason for the lamellar twisting? According to Patel and Bassett (54), the answer is the asymmetricity generated by the uniformly inclined fold surface. The delayed fold surface ordering occurring at lower temperatures leads to the deformation of the planar to the S-shaped sheet. The axis of the 'S', according to Patel and Bassett (54), is inclined with respect to the **b** axis. This will cause the lamella to make a twist about the **b** axis. This twist will be amplified at the screw dislocations because the torsional rigidity is lower at these sites due to the reduced crystal width. Patel and Bassett (54) explained the well-known decrease in band spacing with decreasing crystallization temperature in terms of the lower torsional rigidity and the lower yield stress of thinner crystals formed at lower crystallization temperatures.